Assembly of Smooth Muscle Myosin Minifilaments: Effects of Phosphorylation and Nucleotide Binding

Kathleen M. Trybus and Susan Lowey

Rosenstiel Basic Medical Sciences Research Center, Brandeis University, Waltham, Massachusetts 02254

Abstract. Small bipolar filaments, or "minifilaments," are formed when smooth muscle myosin is dialyzed against low ionic strength pyrophosphate or citrate/Tris buffers. Unlike synthetic filaments formed at approximately physiological ionic conditions, minifilaments are homogeneous as indicated by their hypersharp boundary during sedimentation velocity. Electron microscopy and hydrodynamic techniques were used to show that 20–22S smooth muscle myosin minifilaments are 380 nm long and composed of 12–14 molecules. By varying solvents, a continuum of different size polymers in the range of 15–30S could be obtained. Skeletal muscle myosin, in contrast, preferentially forms a stable 32S minifilament (Reisler, E., P. Cheung, and N. Borochov. 1986. *Biophys. J.* 49:335–342), suggesting underlying differences in the assembly properties of the two myosins. Addition of salt to the smooth muscle myosin minifilaments caused unidirectional growth into a longer "side-polar" type of filament, whereas bipolar filaments were consistently formed by skeletal muscle myosin. As with synthetic filaments, addition of 1 mM MgATP caused dephosphorylated minifilaments to dissociate to a mixture of folded monomers and dimers. Phosphorylation of the regulatory light chain prevented disassembly by nucleotide, even though it had no detectable effect on the structure of the minifilament. These results suggest that differences in filament stability as a result of phosphorylation are due largely to conformational changes occurring in the myosin head, and are not due to differences in filament packing.

It is generally believed that smooth muscles contract by a sliding filament mechanism similar to that existing in striated muscles. The thick and thin filaments lack, however, the regular arrangement found in striated muscles, and there are relatively few myosin filaments compared to the large number of actin filaments (Somlyo, 1980). Although the myosin in smooth muscle cells is structurally very similar to that in skeletal muscles, there are fundamental differences in solubility as described below. These differences account for the extreme lability of myosin filaments in smooth muscles, which for many years made it difficult even to demonstrate their existence. With improved fixation techniques, thick filaments were observed in sections of smooth muscles (Ashton et al., 1975), but native thick filaments are still difficult to isolate by the standard approaches used for skeletal filaments.

The molecular basis for the instability of smooth muscle myosin filaments was discovered by Suzuki et al. (1978). They showed that addition of stoichiometric amounts of MgATP to synthetic filaments formed from dephosphorylated myosin caused them to depolymerize. The disassembled monomers adopt a conformation unique to smooth and nonmuscle myosins, namely the 150-nm-long rod region is folded back upon itself into approximately equal thirds (Onishi and Wakabayashi, 1982; Trybus et al., 1982; Craig et al., 1983). If the regulatory light chain in the myosin head is phosphorylated, however, intermolecular interactions predominate and the filaments remain assembled even in the presence of millimolar nucleotide. These observations were surprising because the rod, and not the head region of myosin, had always been thought to be the principal determinant of filament stability.

In order to examine in more detail how events occurring in the myosin head might affect assembly, it would be advantageous to have a homogeneous population of filaments with a low critical concentration. Synthetic filaments formed by dialyzing monomeric smooth muscle myosin from high salt into solutions of approximately physiological ionic strength are polydisperse, and small changes in the polymer would be difficult to detect. Based on results obtained with skeletal myosin, citrate/Tris was chosen as a desirable buffer for filament formation, because rabbit skeletal muscle myosin assembles into homogeneous small bipolar aggregates, or "minifilaments" in this solvent (Reisler et al., 1980). Because the asembly properties of smooth and skeletal muscle myosin differ, it was not known if smooth muscle myosin could form a minifilament type of structure. Here we show that myosin isolated from either the calf aorta or from turkey gizzards readily assembles into bipolar aggregates, not only in citrate/Tris buffer, but also in pyrophosphate buffer under conditions where skeletal myosin is predominantly monomeric (Reisler et al., 1986*b*).

Although smooth and skeletal muscle myosin both form small oligomers in citrate/Tris buffers, there are important differences between the two systems. Smooth muscle myosin minifilaments do not appear to be a single species, but rather a continuum of polymers ranging in sedimentation from 15 to 30S. This contrasts with the 32S species composed of 16–18 molecules that is considered to be the major stable minifilament formed by skeletal muscle myosin. It has been proposed that this species may correspond, in part, to the central nucleating region of the native bipolar filament (Reisler et al., 1980). Differences in assembly between smooth and skeletal muscle myosin have been recognized ever since ribbon-shaped structures of unusual polarity were observed in sectioned smooth muscle (Small and Squire, 1972). In vitro studies later showed that unlike skeletal muscle myosin, which exclusively forms bipolar filaments, smooth muscle myosin can form either bipolar or "side-polar" filaments. In side-polar filaments, molecules interact in an antiparallel fashion along the entire length of the filament, and not just in the bare zone region (Craig and Megerman, 1977; Hinssen et al., 1978). The type of filament formed by smooth muscle myosin in vivo remains controversial. Crossbridge preservation in sectioned material is too poor to distinguish the polarity of the filaments; moreover, the structure of the filaments may be altered during fixation due to their extreme fragility.

Perhaps the most striking contrast between smooth and skeletal muscle minifilaments lies in the effect of nucleotide on their structure, paralleling the differences observed previously with synthetic filaments (Harrington and Himmelfarb, 1972; Suzuki et al., 1978). As much as 10 mM ATP was needed to completely dissociate myosin or rod minifilaments prepared from skeletal muscle myosin (Oriol-Audit et al., 1981). In this system the ligand acts by binding to low-affinity sites on the rod portion of myosin. The addition of Mg^{2+} depressed the ATP-induced depolymerization, further supporting the conclusion that binding of MgATP to the active site in the head had no effect on the dissociation (Oriol-Audit et al., 1981). The opposite results have been obtained here with minifilaments prepared from smooth muscle myosin: <1 mM MgATP was sufficient to fully dissociate the minifilaments, provided that the myosin was dephosphorylated. Phosphorylated minifilaments, as well as rod minifilaments, remained assembled, consistent with a system where nucleotide acts through the head region of myosin.

Because of the small size and homogeneity of the minifilaments, we have been able to show that phosphorylation has no effect on the structural organization of the minifilaments, and therefore the instability introduced by nucleotide binding must be attributed to conformational changes occurring in the myosin head. In the accompanying article, experiments aimed at showing how such changes can lead to disassembly of the smooth muscle myosin filament are described.

Materials and Methods

Protein Preparation

Smooth muscle myosin from calf aortas was purified by the method of Megerman and Lowey (1981) with the modifications described in Trybus et al. (1982). Turkey gizzard myosin was prepared as described by Sellers et al. (1981). The method described in Margossian and Lowey (1982) was used for the preparation of chicken pectoralis myosin. Smooth muscle myosin light chain kinase was isolated according to Adelstein and Klee (1981) with the exception of the first gel filtration column. Calmodulin was a gift from C. Klee (National Institutes of Health, Bethesda, MD). Protein concentrations were determined using $E^{1\%}_{280} = 4.8$ for the column-purified calf aorta myosin, and $E^{1\%}_{280} = 5.0$ for turkey gizzard and skeletal myosin. A molecular weight of 500,000 was used for all myosins. Smooth muscle myosin was thiophosphorylated in low ionic strength buffer as previously described (Trybus and Lowey, 1984).

Preparation of Rod

Myosin in 0.2 M ammonium acetate, pH 7.2, was digested to subfragment-1 and rod with papain. The rod fraction was purified by ethanol fractionation (Margossian and Lowey, 1982). Protein concentration was determined by interference optics using an analytical ultracentrifuge (model E, Beckman Instruments, Inc., Fullerton, CA), assuming four fringes per milligram per milliliter of protein. The extinction coefficient of the turkey gizzard rod calculated from a fringe count and absorption spectrum was $E^{1\%}_{280} = 0.86$. The tyrosine content of the rod was determined from the absorption spectrum in 0.1 N HCl (E = 1,340/M. cm, 274.5 nm) and 0.1 N NaOH (E = 2,330/M.cm, 293.5 nm) (Beaven and Holiday, 1952). The value of 5–6 mol Tyr/110,000-g rod that was obtained by this method agreed reasonably well with that determined from the amino acid composition of a 24-h hydrolysate, which was 4.7 mol Tyr/110,000-g (model D500 analyzer, Durrum, Palo Alto, CA). The number of tryptophans per chain of the rod is therefore limited to a maximum of one, based on the total extinction coefficient and that calculated for five to six tryosines.

Citrate/Tris Buffers

Citrate/Tris solutions were prepared by titrating citric acid with Tris base until the pH of the solution was 8.05 at 4°C. The final composition of the solutions was 2 mM citrate/11 mM Tris, 5 mM citrate/22 mM Tris, 10 mM citrate/41 mM Tris, and 20 mM citrate/90 mM Tris. The Tris concentration was not varied to compensate for pH changes with temperature; thus if the minifilaments were used at 20°C the pH of the 5 mM citrate/22 mM Tris solution decreased to ~7.65.

Cross-linking

1 mg/ml myosin or rod minifilaments were cross-linked with freshly prepared solutions of dimethylsuberimidate (Pierce Chemical Co., Rockford, IL) for varying lengths of time (0–120 min) on ice. A low-protein concentration was required to maximize cross-linking within instead of between minifilaments. The final concentration of dimethylsuberimidate was typically 3–6 mg/ml for cross-linking minifilaments in 5 mM pyrophosphate, pH 7.5, and 0.25–1.5 mg/ml for cross-linking minifilaments at the higher pH of the 5 mM citrate/Tris buffer. If samples were only used for SDS-gel electrophoresis, the reaction was stopped either by addition of 0.33 M ethanolamine, pH 8, or 20 mM ammonium acetate, pH 7.2. Ethanolamine caused cross-linked and uncross-linked minifilaments to aggregate, and therefore was not used to stop the reaction if the minifilaments were used for solution studies. In most cases, the cross-linking reaction was terminated by dialyzing out the excess dimethylsuberimidate or by removing the cross-linking reagent by gel filtration on Sephadex G-50 (Pharmacia Fine Chemicals, Piscataway, NJ), which had been depleted of its void volume buffer by centrifugation (Neal and Florini, 1973). In pyrophosphate, cross-linking conditions were chosen based on the following criteria: the turbidity of the cross-linked sample should be the same as control filaments, and bands greater than 400,000 mol wt should be resolved on 2.5% acrylamide gels. In citrate/Tris, the extent to which the filaments were cross-linked prior to shadowing was followed by the decreasing ability of 1 mM MgATP to dissociate the dephosphorylated filament to the 15S species. Cross-linking conditions where MgATP had little or no dissociating effect could be obtained. Cross-linked filaments sedimented at essentially the same rate as unmodified filaments; over-cross-linking typically results in formation of very large aggregates that rapidly sedimented at low speed. Minifilaments with only slightly larger sedimentation coefficients were not formed, suggesting that the filaments visualized by microscopy are the 22S species observed in solution in 5 mM citrate/22 mM Tris.

Gel Electrophoresis

Dephosphorylated and phosphorylated regulatory light chains were separated on glycerol/acrylamide gels (Perrie and Perry, 1970) as described in Trybus and Lowey (1984). SDS gel electrophoresis was performed according to the method of Laemmli (1970). Cross-linked minifilaments were sepa-

rated on SDS slab gels composed of 2.5% acrylamide and 0.5% agarose (acrylamide/bisacrylamide ratio of 37.5:1). A stacking gel of lower pH and porosity was not used.

Viscosity

Viscosity was measured in Ostwald-type viscometers with flow times of 120 s for buffer at 20°C. The minifilaments were clarified for 15 min at 10,000 *g* before the viscosity measurements.

Centrifugation

Sedimentation velocity measurements were carried out at 20°C in a Beckman model E analytical ultracentrifuge, using the schlieren optical system. Bar angle was 60°. It should be noted that, in the text, intrinsic sedimentation coefficients ($s_{20,w}$ extrapolated to zero protein concentration) are typically referred to. In figures, however, the reported sedimentation rates are usually given at a finite protein concentration, which, for asymmetric proteins, are less than the intrinsic coefficient.

Electron Microscopy

Electron microscopy was performed on a Philips EM301 electron microscope operated at 60 kV for rotary shadowing or 80 kV for negatively stained images. Magnification was calibrated using the 39.5-nm repeat of tropomyosin paracrystals. Minifilament samples were rotary shadowed with platinum by the method of Tyler and Branton (1980) as described in Trybus and Lowey (1984). The minifilaments were diluted either into 5 mM pyrophosphate, pH 7.5/66% glycerol or 0.5 M ammonium acetate, pH 7.2/66% glycerol before spraying the sample onto mica, as described in the text. For negative staining, a drop of filaments (25–50 μg/ml) was placed on a UV-irradiated carbon-formvar grid for ~30 s. The grid was then washed with 5 drops of filament buffer followed by 5 drops of 1% uranyl acetate. Excess stain was removed and the grids were air-dried at room temperature.

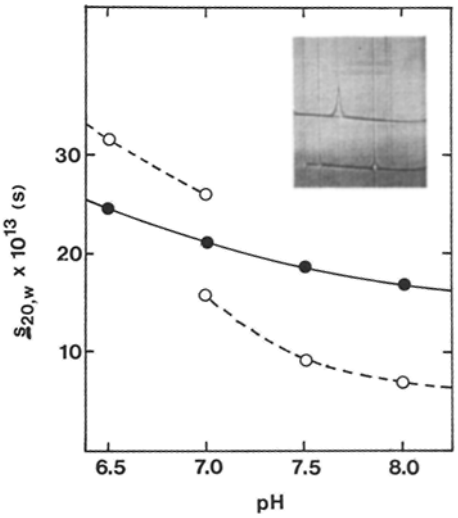

Figure 1. Sedimentation of smooth and skeletal muscle myosin in 5 mM pyrophosphate. The sedimentation coefficients (*s*) of (●) smooth muscle myosin and (○) chicken pectoralis myosin in 5 mM pyrophosphate are plotted as a function of pH. Smooth muscle myosin forms minifilaments at pH 6.5–8. Skeletal myosin begins to dissociate at pH 7; the sedimentation coefficient approaches the value for monomeric myosin as the pH is increased. Protein concentration: 0.15 mg/ml turkey gizzard myosin, 0.4 mg/ml chicken pectoralis myosin. (*Inset*) Sedimentation pattern of skeletal (*upper, broad boundary*) and smooth muscle myosin (*lower, hypersharp boundary*) in 5 mM pyrophosphate, pH 8. Protein concentration, 1.5 mg/ml.

Results

Smooth Muscle Myosin Forms Minifilaments in Pyrophosphate

Skeletal myosin minifilaments are typically prepared by a two-step procedure: the myosin is first solubilized as monomers and dimers in a low ionic strength, high pH pyrophosphate buffer (5 mM, pH 8), and then dialyzed against 10 mM citrate/Tris, pH 8 (Reisler et al., 1980). When smooth muscle myosin isolated from calf aortas was similarly dialyzed into pyrophosphate, sedimentation velocity experiments showed that the myosin was not in the 6S monomeric form, but instead sedimented as a faster hypersharp boundary (Fig. 1, *inset*). This sedimentation profile is characteristic of a homogeneous population of asymmetric molecules. Both smooth and skeletal myosin can therefore assemble into minifilament type structures, but the solvent conditions necessary for polymerization differ. As the pH of the pyrophosphate decreased from 8.0 to 6.5, the sedimentation rate of the smooth muscle myosin filaments increased from ~15S to 25S (Fig. 1). Chicken pectoralis myosin can also polymerize in 5 mM pyrophosphate, but only at low pH values. Above pH 7.5, skeletal myosin was predominantly monomeric (Fig. 1) (Reisler et al., 1986*b*). Smooth muscle myosin minifilaments could only be solubilized by increasing the pyrophosphate concentration to 40 mM pyrophosphate, pH 7.5, where the ionic strength is ~0.28 M.

Phosphorylation of the myosin regulatory light chain had no apparent effect on filament assembly in pyrophosphate. Fig. 2 shows that regardless of whether minifilaments were formed from completely phosphorylated or dephosphorylated myosin, a minifilament with an intrinsic sedimentation coefficient of 20.2S was formed in 5 mM pyrophosphate, pH 7.5. Rod interactions thus appear to determine the type of filament that is formed in the absence of nucleotide. Consistent with these findings, the rod alone assembled into minifilaments, as indicated by a hypersharp boundary during sedimentation velocity, and by the appearance of the metal-shadowed filaments by electron microscopy (see Fig. 5).

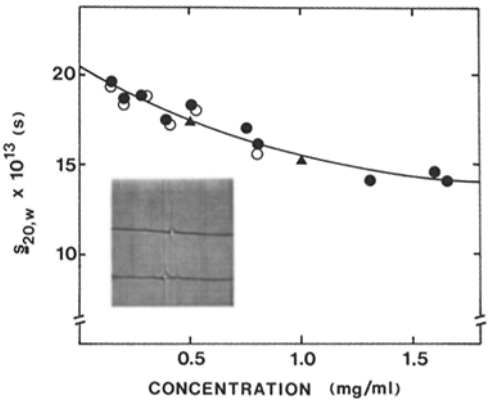

Figure 2. Phosphorylated and dephosphorylated myosin form the same minifilament. The sedimentation coefficients (*s*) of (○) phosphorylated and (●) dephosphorylated calf aorta myosin in 5 mM pyrophosphate, pH 7.5, are plotted as a function of protein concentration. Extrapolated to infinite dilution, the sedimentation coefficient of both species is 20.2S. (▲) Dephosphorylated turkey gizzard myosin assembles into the same structure. (*Inset*) Sedimentation pattern of (*upper*) 0.8 mg/ml and (*lower*) 1.6 mg/ml myosin.

Figure 3. Electron micrograph of metal-shadowed minifilaments. 20S minifilaments formed from calf aorta myosin (5 mM pyrophosphate, pH 7.5) were cross-linked and then metal-shadowed in 5 mM pyrophosphate pH 7.5/66% glycerol. The average number of molecules per filament was 13–14, and the average filament length was 393 ± 33 nm. Note the presence of several folded 10S monomers in the background. Bar, 0.1 μm.

Size and Shape of 20S Minifilaments by Electron Microscopy

The length and number of molecules in a given species, such as the 20S minifilament formed in 5 mM pyrophosphate, pH 7.5, could be examined in more detail by electron microscopy. Before direct visualization, however, it was necessary to cross-link the minifilaments with dimethylsuberimidate in order to prevent the native structure from disassembling during processing for rotary shadowing (see Materials and Methods). The minifilaments observed in the electron microscope were bipolar, and quite homogeneous in size and shape (Fig. 3). Some variability in size would be expected, in that filaments that are not completely cross-linked can disassemble. Moreover, every filament in solution is probably not composed of an identical number of molecules. These images of platinum-shadowed minifilaments are sufficiently well resolved to allow the number of molecules per filament to be counted. As shown in the histogram in Fig. 4 *A* (*left*), the average number of molecules on each side of the bipolar filament was 6.8 ± 1.8 (n = 128), indicating that an average filament is composed of 13–14 molecules. If the filaments were not cross-linked before shadowing, the average number of molecules per filament decreased to 8.8 (n = 65), but 52% of the filaments had five molecules per side. A minimum estimate of 10 molecules per 20S filament can therefore be established by these experiments. The total length of the cross-linked filament, which included the most distal heads on both sides of the filament, was 393 ± 33 nm (n = 78), and the bare zone length was 177 ± 26 nm (n = 66) (Fig. 4 *A*, *right*). A feature of the myosin head that was apparent in a number of molecules was the presence of a third region of metal accumulation at the neck. This might be due to the regulatory light chains which have been localized to this region of the head in other myosins (Vibert and Craig, 1982; Walzthöny et al., 1984).

Metal-shadowed images of the rod polymer confirmed what had been implied by the sedimentation velocity experiments, namely, this proteolytic fragment formed structures very similar to those observed with whole myosin (Fig. 5). The average length of the rod minifilaments was 375 ± 39 nm (n = 87), in good agreement with the value obtained after subtracting the length of the head region from the average length of the myosin minifilaments. This result was not necessarily expected, because in more typical filament-forming buffers (0.15 M KCl, 10 mM phosphate, pH 7.5), myosin and rod polymerized quite differently.

Uncross-linked, metal-shadowed minifilaments not only provided a minimum estimate of the number of molecules in the polymer, but also revealed smaller structures such as dimers and tetramers that resulted from filament disassembly. Although these oligomers are not necessarily intermediates in the assembly pathway of minifilaments, they do highlight certain favored interactions between molecules. Fig. 6 illustrates some of these structures: parallel dimers that are either not staggered or staggered by less than the length of a head (*B*); parallel dimers with an axial translation of 40–

50 nm (*C*); antiparallel dimers or tetramers that have 40–50-nm overlaps (*D*). The relative abundance of these three dimeric species, which account for <10% of the molecules in the field, was estimated at 65%, 15%, and 20%, respectively. The smaller size of the uncross-linked minifilaments compared with the cross-linked species allows certain features to be seen more easily as illustrated in Fig. 6, *E* and *F*. Some polymers have two levels of crossbridges on each side of the filament, whereas others have three; the heads at one level are often separated by 40–50 nm from molecules at the next level. Some molecules appear to be staggered by less than this distance, but the flexibility of the head at the head-rod junction causes some heads to bend back towards

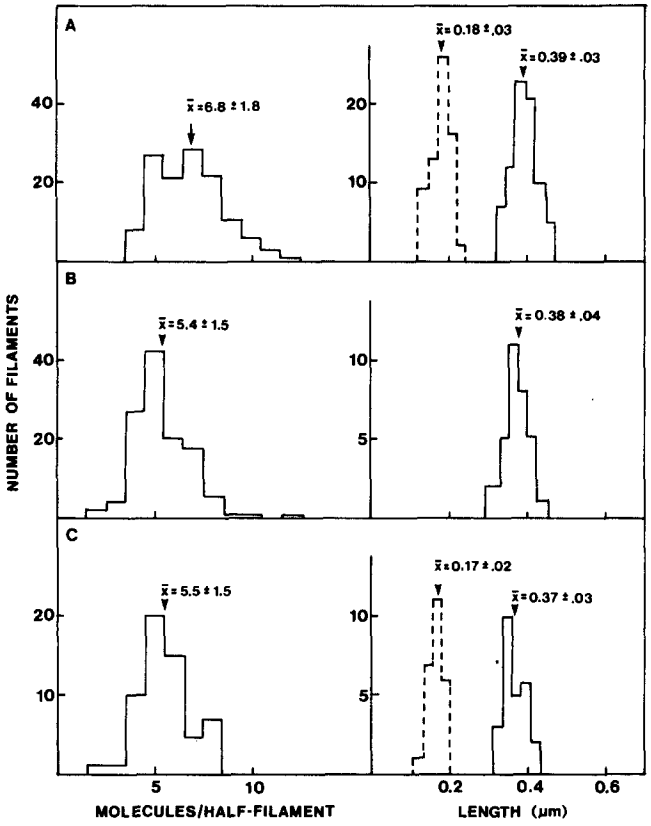

Figure 4. Histograms showing the number of molecules per half-filament and the distribution of filament and bare-zone lengths. (*A*) 20S minifilaments formed from calf aorta myosin (5 mM pyrophosphate, pH 7.5) were cross-linked and then rotary-shadowed in 5 mM pyrophosphate, pH 7.5/66% glycerol. The average number of molecules per side of the filament was 6.8 ± 1.8 (n = 128), the total length 393 ± 33 nm (n = 78), and the bare zone length 177 ± 26 nm (n = 66). (*B*) 22S turkey gizzard myosin minifilaments (5 mM citrate/22 mM Tris) were cross-linked and then diluted into 0.5 M ammonium acetate/66% glycerol for shadowing to provide a minimum estimate of the number of molecules per filament. The number of molecules per half-filament was 5.4 ± 1.5 (n = 124), and the length was 378 ± 35 nm (n = 35). (*C*) Same as *B* except that the cross-linked filaments were diluted into 5 mM pyrophosphate, pH 7.5/66% glycerol for shadowing. This solvent considerably reduced the number of large aggregates observed when cross-linked minifilaments were diluted into ammonium acetate. The number of molecules per half-filament was 5.5 ± 1.3 (n = 57), the total length 369 ± 30 nm (n = 28), and the bare zone length 168 ± 21 nm (n = 25).

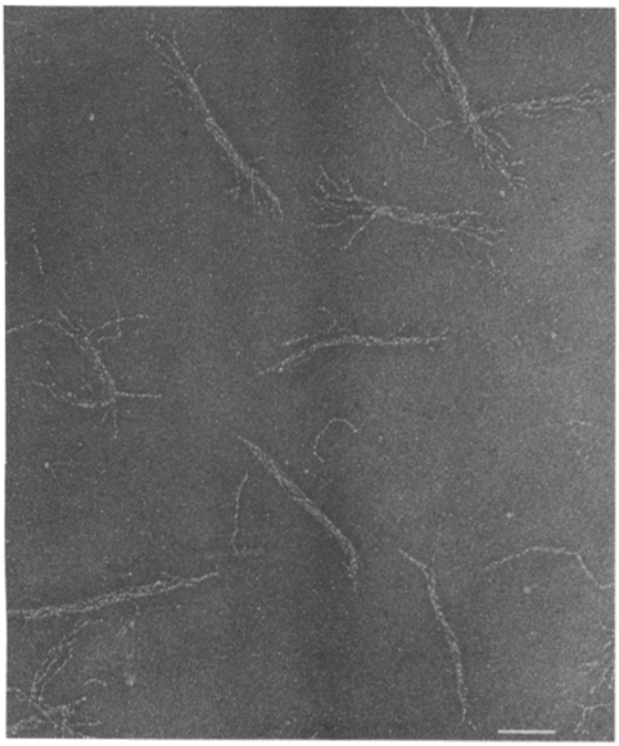

Figure 5. Electron micrograph of metal-shadowed rod minifilaments. Rod prepared from calf aorta myosin assembled into structures similar in size and shape to those formed by intact myosin (5 mM pyrophosphate, pH 7.5; see Fig. 3). The average total length of these minifilaments was 375 ± 39 nm, only slightly shorter than the value obtained with myosin minifilaments. Bar, 0.1 μm.

the rod and others to bend away from the rod, thereby obscuring the interpretation. Moreover, the molecules are often splayed away from the filament backbone, and it is difficult to determine the exact spacing between adjacent levels of heads. The number of molecules at each level varies from one to three, but generally decreases with distance from the bare zone. The overall picture that emerges from these measurements is of a filament with two to three levels of crossbridges, staggered most likely by 43 nm, on either side of an ~170-nm-long bare zone.

Minifilament Formation in Citrate/Tris

Pyrophosphate is the preferred solvent for resolving details of the minifilament structure by electron microscopy, but it is not a suitable solvent for determining the effect of MgATP on filament stability, or for measuring enzymatic activity, because this ligand competes with MgATP for the active site. A solvent such as citrate/Tris, in which skeletal myosin forms minifilaments (Reisler et al., 1980), is more suitable for experiments that require the use of nucleotide. Following the procedure used to generate skeletal muscle myosin minifilaments, calf aorta or chicken gizzard myosin in 5 mM pyrophosphate, pH 7.5 (where it is filamentous) or in 40 mM pyrophosphate, pH 8.5 (where it is monomeric) was dialyzed against citrate/Tris. Although the properties of myosin isolated from the gizzard or the aorta were the same in pyrophosphate (Fig. 2), only turkey gizzard myosin gave a single hypersharp peak in citrate/Tris. Differences between smooth

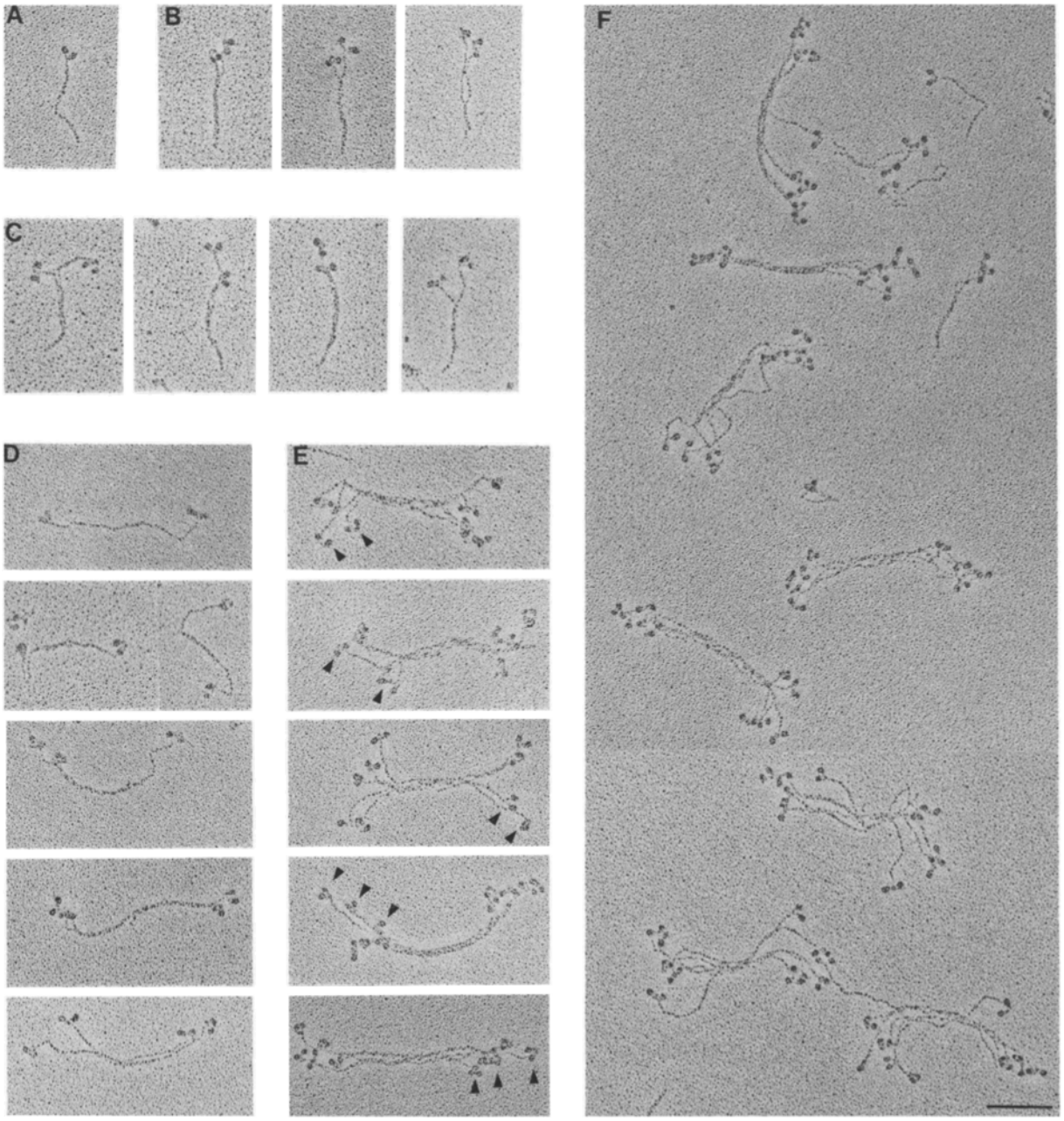

Figure 6. Electron micrographs of uncross-linked minifilaments. These images were observed in fields of uncross-linked minifilaments (5 mM pyrophosphate, pH 7.5), and might represent intermediates in the assembly pathway. (*A*) Myosin monomer for comparison; (*B*) parallel dimers that are either not staggered or staggered by less than the length of the head; (*C*) parallel dimers with an axial translation of 40–50 nm; (*D*) antiparallel dimers or tetramers with 40–50-nm overlaps; (*E*) minifilaments that illustrate the variable number of molecules (one to three) per level, and that clearly show two or three levels of molecules per side, staggered by 40–50 nm. (*F*) A field of uncross-linked 20S minifilaments. Bar, 0.1 μm.

muscle myosins isolated from mammalian and avian sources have been previously observed in the salt dependence of their conformational transitions (Trybus and Lowey, 1984). With both myosins, the minifilaments formed in a given solvent were independent of the pathway by which the polymer was obtained. For simplicity, minifilaments were typically formed by dialysis from 0.6 M KCl directly into citrate/Tris. This assembly behavior contrasts with that of synthetic filaments whose size usually depends on factors such as the speed of dilution from the higher to the lower ionic strength buffer.

The 22S minifilaments formed in 5 mM citrate/22 mM Tris were characterized by electron microscopy. Citrate/Tris unfortunately proved to be a poor solvent for shadowing, in that structural details were obscured in this solvent. Cross-linked filaments had to be diluted either into 0.5 M ammonium acetate, pH 7.2, or into a low ionic strength pyrophosphate buffer just before spraying the sample onto mica for shadowing. Dilution of the cross-linked filaments into ammonium acetate provides a minimum estimate of the number of molecules per filament, because some uncross-linked

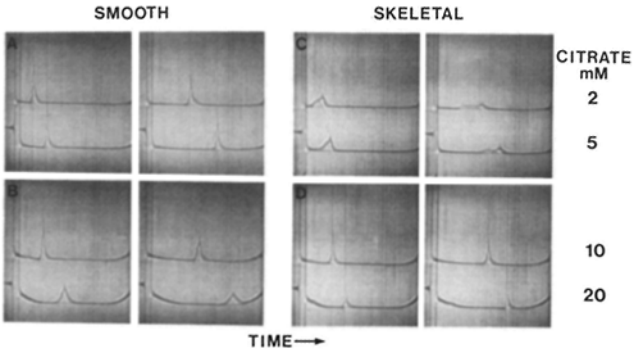

Figure 7. Sedimentation patterns of smooth and skeletal myosin in 2–20 mM citrate/Tris buffer. The sedimentation patterns of (*A* and *B*) turkey gizzard myosin and (*C* and *D*) chicken pectoralis myosin in 2, 5, 10, and 20 mM citrate/Tris, pH 7.6, 20°C. The two patterns at each citrate concentration were taken at different times (*A* and *C*, 18 and 50 min; *B* and *D*, 17 and 31 min). The shape of the boundary at any given citrate concentration is quite different for the two myosins. The sedimentation coefficients listed in order of increasing citrate concentration were 15.8, 19.4, 24.2, and 37.3 for turkey gizzard myosin minifilaments and 14.2, 19.2, 25.0, and 31.6 for the chicken pectoralis myosin polymers. The minifilaments from both myosins were formed by the two-step procedure; namely, they were first dialyzed into pyrophosphate and then into citrate/Tris. Protein concentration, 0.5 mg/ml; 30-mm cells; rotor speed, 40,000 rpm.

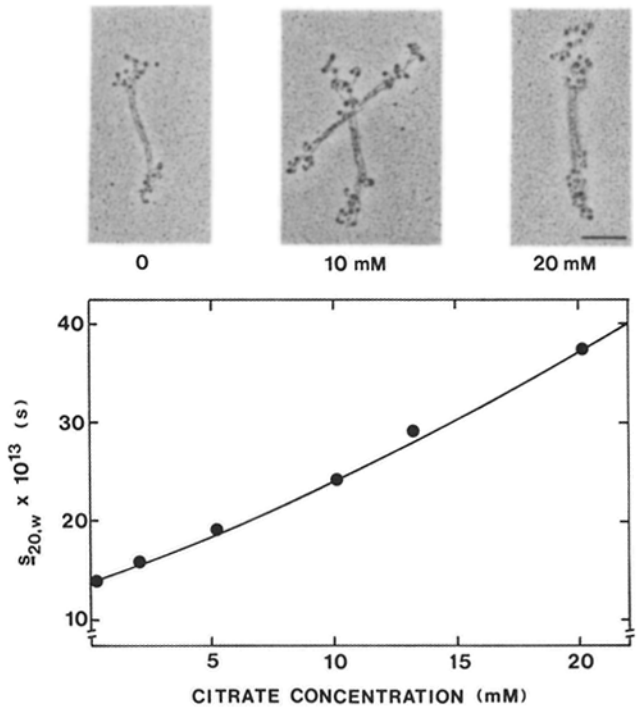

Figure 8. Sedimentation coefficients (*s*) and electron micrographs of minifilaments formed in varying citrate concentrations. The sedimentation coefficients of 0.5 mg/ml turkey gizzard myosin minifilaments gradually increase with the citrate/Tris (pH 7.6) concentration. Although not plotted here, the sedimentation coefficients extrapolated to zero protein concentration are 22.2, 29.0, and 33.5S in 5, 10, and 13 mM citrate/Tris, respectively. The upper part of the figure shows electron micrographs of minifilaments formed at the indicated citrate concentrations. The number of molecules per filament is clearly increasing; the width appears to be changing more than the length. Bar, 0.1 μm.

molecules dissociated to monomer. The histogram in Fig. 4 *B* shows that the average number of molecules per half filament was 5.4 ± 1.5 (n = 124) and the average length was 378 ± 38 nm (n = 35). Similar values for the length and number of molecules were obtained if the cross-linked filaments were diluted into pyrophosphate for shadowing (Fig. 4 *C*). This favorable solvent largely eliminated the aggregation problems caused by ammonium acetate and also allowed measurement of the length of the bare zone, which was 168 ± 21 nm (n = 25). The 22S filaments formed in citrate/Tris are thus quite similar to the 20S filaments formed in pyrophosphate.

Comparison of Smooth and Skeletal Myosin Minifilaments in Citrate/Tris

The polymers formed by turkey gizzard myosin in 2, 5, 10, and 20 mM citrate/Tris (Fig. 7, *A* and *B*) were compared with the species formed by chicken pectoralis myosin in these same solvents (Fig. 7, *C* and *D*). Although the sedimentation coefficients of the smooth and skeletal filaments are similar below 15 mM citrate, the shapes of the sedimenting boundaries suggest that different structures have been formed. At 2 and 5 mM citrate/Tris, smooth muscle myosin minifilaments are completely assembled and sedimented as a hypersharp boundary even at concentrations as low as 0.5 mg/ml, whereas skeletal filaments are partially dissociated as indicated by the polydisperse boundary. A single boundary is observed for both myosins in 10 and 20 mM citrate/Tris, but the sedimenting boundary of the smooth muscle myosin filaments is much broader than that of the skeletal muscle myosin minifilaments.

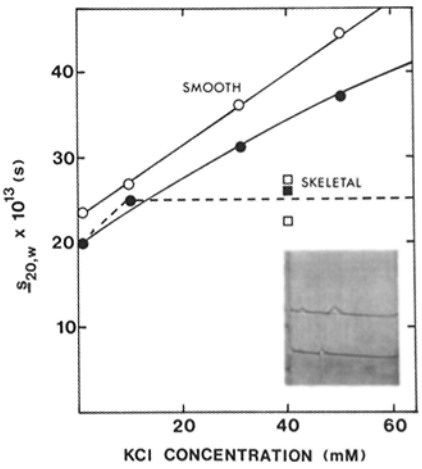

Figure 9. Growth of minifilaments upon addition of salt. The sedimentation coefficients (*s*) of the polymers formed upon addition of varying KCl concentration to turkey gizzard myosin minifilaments (1 mg/ml) are indicated (●, 5 mM citrate/Tris; ○, 10 mM citrate/Tris). For comparison, the dashed line shows the species that would be formed by rabbit skeletal myosin minifilaments in 5 mM citrate/Tris (taken from Reisler et al., 1986*a*). The polymers formed by adding 40 mM KCl to chicken pectoralis minifilaments are also shown (■, 5 mM citrate/Tris; □, 10 mM citrate/Tris). (*Inset*) Sedimentation pattern of polymers formed after a 24-h incubation of (*upper*) smooth or (*lower*) skeletal myosin minifilaments (10 mM citrate/Tris) with 40 mM KCl.

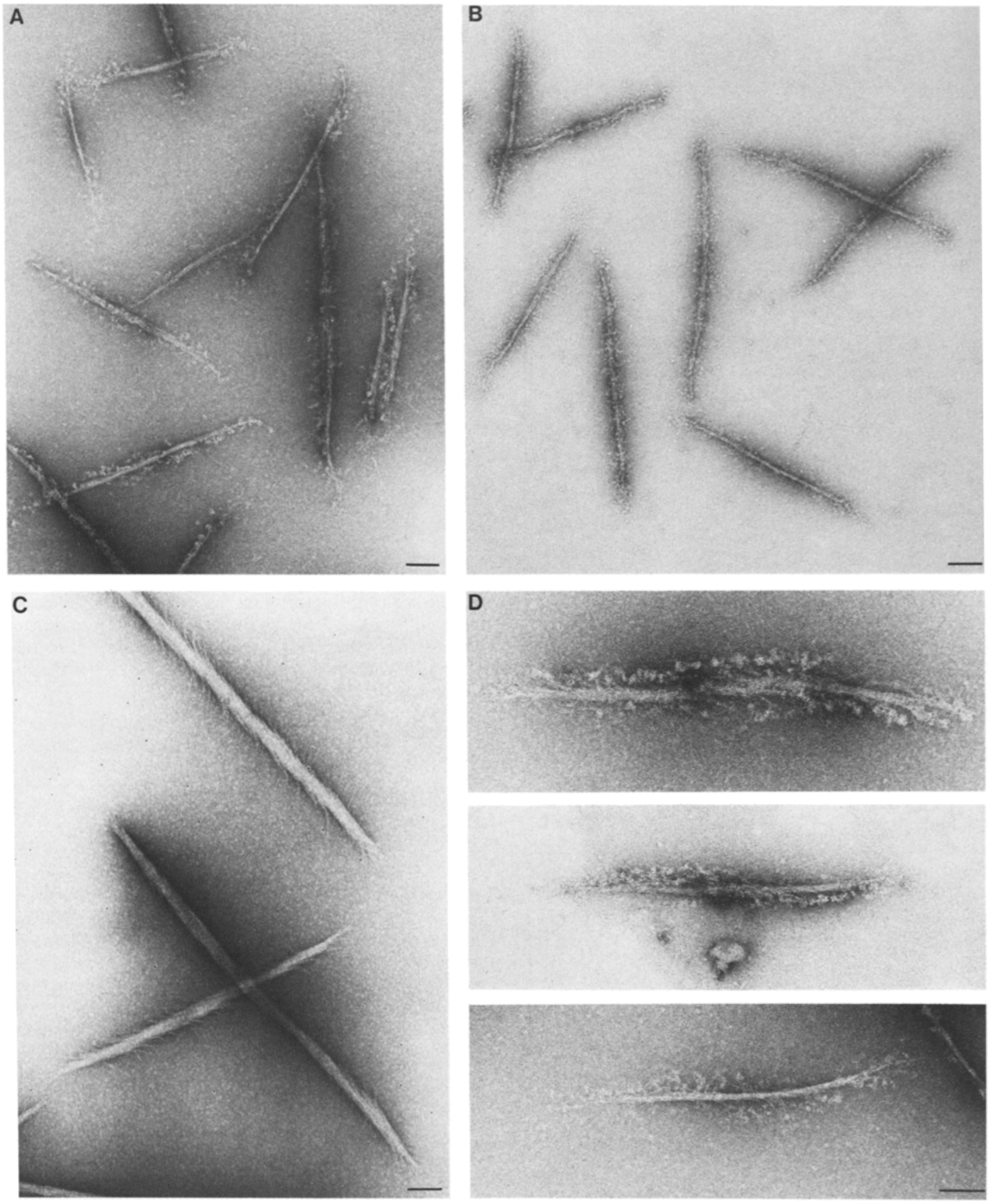

Figure 10. A comparison of filaments formed from smooth and skeletal muscle myosin. The filaments formed by addition of 0.1 M KCl to (*A* and *D*) smooth muscle or (*B*) skeletal muscle myosin minifilaments in 5 mM citrate/16 mM Tris have different morphologies, indicating that the two types of myosin have different preferred modes of packing. (*C*) Smooth muscle myosin rod forms filaments with a distinct side-polar morphology. Bar, 0.1 μm.

The sedimentation rate of gizzard myosin minifilaments increased continuously with increasing citrate/Tris concentration (Fig. 8). The sedimentation coefficients of the chicken pectoralis myosin filaments also increased with citrate concentration, although at 20 mM citrate/Tris the value was slightly lower than that obtained for the smooth muscle minifilaments. The images of the metal-shadowed smooth muscle myosin filaments formed in different citrate/Tris concentrations show that the filaments appear to be growing more in width than in length (Fig. 8). The formation of a less asymmetric polymer is consistent with the broadening of the sedimenting boundary as the citrate concentration is raised (Fig. 7).

The effect of salt on the growth of smooth and skeletal myosin minifilaments was also examined (Fig. 9). Small additions of KCl (10–20 mM) to 18S (2 mM citrate/Tris) and 22S (5 mM citrate/Tris) rabbit skeletal myosin minifilaments cause them to convert to 32S minifilaments (Reisler et al., 1986*a*). The 32S minifilaments then remain stable until the salt concentration exceeds ~70 mM, whereupon the minifilaments rapidly grow into larger filaments between 0.1 and 0.15 M KCl (Reisler et al., 1982). Both 22S (5 mM citrate/Tris) and 29S (10 mM citrate/Tris) smooth muscle myosin minifilaments, in contrast, increase in sedimentation rate in a continuous fashion as salt is added in the 10–60 mM range (Fig. 9). This result suggests that smooth muscle myosin, unlike skeletal myosin, does not form a particular size filament that is more stable than any other size polymer.

The morphology of the filaments formed when salt was added to smooth and skeletal myosin minifilaments was compared by electron microscopy (Fig. 10). Smooth and skeletal myosin were dialyzed into 5 mM citrate/16 mM Tris, pH 7.4 (4°C) (this lower pH was chosen to favor growth of larger filaments), and the concentration of KCl was increased to 0.1 M. The filaments formed from smooth muscle myosin and chicken pectoralis myosin were similar in length (0.5–1 μm), but the polarity of the crossbridges differed markedly (Fig. 10). The skeletal myosin minifilaments had the typical bipolar structure with myosins oriented in opposite directions from a central region. The smooth muscle myosin minifilaments appeared to have a single orientation of crossbridges along the entire length of one side of the filament, and the opposite polarity along the other side. Bare zones were at the filament ends instead of at the center. This "side-polar" packing was particularly striking in filaments formed by the rod portion of smooth muscle myosin (Fig. 10 *C*). It is clear, therefore, that although certain general features are shared by the minifilaments from smooth and skeletal myosin, the basic mode of assembly is quite different.

Effect of MgATP on Minifilaments

The most striking difference between smooth and skeletal muscle myosin filaments is in the effect of MgATP on the stability of the polymer. In order for smooth muscle myosin minifilaments to be a useful model system for assembly studies, they must be sensitive to the presence of nucleotide and to the degree of regulatory light chain phosphorylation, as is true of synthetic filaments (Suzuki et al., 1978). In the absence of nucleotide, both phosphorylated and dephosphorylated myosin form a 22S minifilament in 5 mM citrate/Tris (Fig. 11, *A* and *C*, *upper patterns* and Fig. 12). It appears that

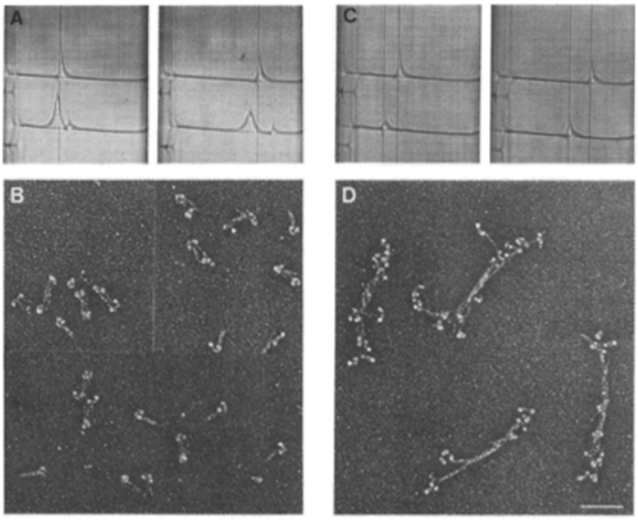

Figure 11. Effect of 1 mM MgATP on dephosphorylated and phosphorylated minifilaments. (*A*) Sedimentation patterns of dephosphorylated minifilaments (5 mM citrate/Tris) in the (*upper*) absence or (*lower*) presence of 1 mM MgATP. >90% of the dephosphorylated filaments are depolymerized to a 15S component. Protein concentration, 1.8 mg/ml. (*B*) Electron micrograph of the species formed after addition of MgATP to dephosphorylated minifilaments; namely, a mixture of folded monomers and antiparallel folded dimers. The 15S species was cross-linked and shadowed in 0.5 M ammonium acetate/66% glycerol. (*C*) Sedimentation patterns of phosphorylated minifilaments in the (*upper*) absence or (*lower*) presence of 1 mM MgATP. Even after nucleotide addition, a monomer peak cannot be detected. The minifilaments sediment more slowly, however, in the presence of MgATP. Protein concentration, 2.1 mg/ml. (*D*) Electron micrograph of phosphorylated minifilaments crosslinked in the presence of MgATP and shadowed in 0.5 M ammonium acetate/66% glycerol. No major structural changes have occurred upon nucleotide addition. Bar, 0.1 μm.

phosphorylation does not affect the structure of the filament in either pyrophosphate (see Fig. 2) or citrate/Tris (Fig. 12). Upon addition of 1 mM MgATP, however, the dephosphorylated minifilaments dissociated to a species that sedimented at 15S (Fig. 11 *A*, *lower pattern*). This species, previously observed in other low ionic strength solvents (Trybus and Lowey, 1984), is a mixture of folded monomers and antiparallel dimers, as shown in the electron micrograph in Fig. 11 *B*. The sedimentation coefficient of the folded species has very little concentration dependence (Fig. 12), consistent with the compact, relatively symmetric shape of the folded dimer.

Even though phosphorylated minifilaments were resistant to the disassembling action of 1 mM MgATP, and showed no evidence of a slower sedimenting boundary (Fig. 11 *C*, *lower pattern*), an effect of nucleotide on the phosphorylated species was evident. At finite concentrations (e.g., 2 mg/ml) the sedimentation coefficient of the phosphorylated filaments decreased by as much as 2S upon nucleotide addition (Fig. 12). The change in sedimentation cannot be due to a small amount of disassembly, because the observed sedimentation coefficient would then be expected to increase. Moreover,

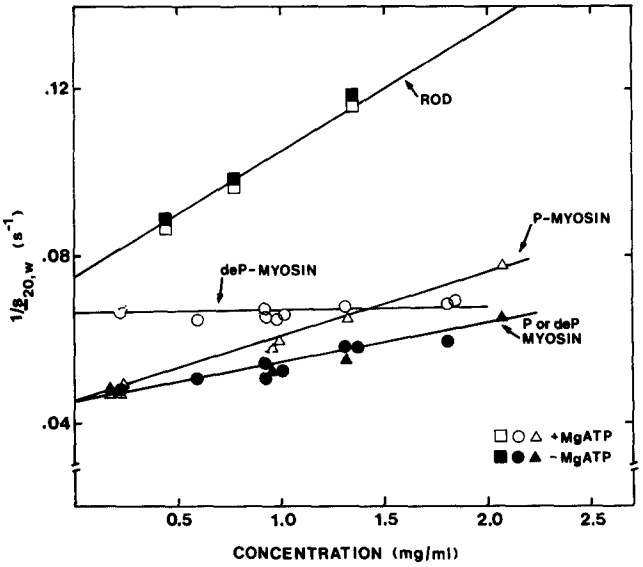

Figure 12. Sedimentation coefficients (*s*) of dephosphorylated, phosphorylated, and rod minifilaments in the presence or absence of 1 mM MgATP. (●, ▲) Dephosphorylated or phosphorylated myosin forms a 22S minifilament (5 mM citrate/Tris) in the absence of MgATP. (○) Upon nucleotide addition, dephosphorylated filaments disassemble to a 15S component, which is a mixture of folded monomers and dimers. (△) 1 mM MgATP does not depolymerize the phosphorylated minifilaments, but the sedimentation coefficient at finite protein concentration is reduced, indicating a change in solute–solvent interactions. Rod minifilaments sediment at the same rate in the (■) absence or (□) presence of 1 mM MgATP.

because the sedimentation coefficients of the filaments converged to the same value of 22S at infinite dilution, it can be assumed that the different slopes in the presence and absence of MgATP are due to thermodynamic interactions between solute and solvent rather than any structural change in the filaments.

Unlike whole myosin, the sedimentation coefficient of rod minifilaments did not change upon addition of 1 mM MgATP (Fig. 12). This result confirmed that effects of nucleotide on filament stability are mediated through the myosin head, and not through the rod as with skeletal myosin. The intrinsic sedimentation coefficient of the rod minifilaments was 13S, approximately half the value obtained with whole myosin. The shape of the myosin and rod minifilaments must be quite similar, inasmuch as the smaller sedimentation coefficient of the rod minifilaments can be accounted for by the twofold decrease in molecular weight of this proteolytic fragment. Similar structures were in fact observed by electron microscopy when rod and myosin minifilaments formed in pyrophosphate were metal-shadowed (compare Figs. 3 and 5).

Viscosity measurements confirmed that MgATP had an effect on phosphorylated myosin minifilaments, but not on rod minifilaments. When $\eta sp/c$ was plotted as a function of concentration for the phosphorylated minifilaments, the slope was fivefold lower in the presence of 1 mM MgATP than in its absence (data not shown). The steep concentration dependence found in the absence of nucleotide indicates strong solute–solvent interactions. Although nucleotide caused a decrease in viscosity at finite concentrations, the intrinsic viscosity of phosphorylated minifilaments at infinite dilution remained the same whether or not nucleotide was present. The viscosity of rod minifilaments, like the sedimentation coefficient, was unaffected by 1 mM MgATP at all concentrations. The invariance of both the intrinsic viscosity and the intrinsic sedimentation coefficient strengthens the argument that the phosphorylated filament is not disassembled by nucleotide under these ionic conditions.

Discussion

Myosin assembles into thick filaments in both muscle and nonmuscle cells. In striated muscle, the myosin filaments are stable, bipolar structures. In nonmuscle cells, myosin filaments are difficult to detect, but are believed to mediate cell movements by an assembly/disassembly cycle in response to certain signals (Yumura and Fukui, 1985). At one time it was hypothesized that myosin in resting smooth muscles was soluble and assembled into filaments only during contraction (Shoenberg, 1969). With the development of improved fixation techniques, including rapid freezing, this has now been disproved and myosin filaments have been demonstrated in both the relaxed and contracted state (Somlyo et al., 1981). The remarkable effect of MgATP and phosphorylation on the stability of smooth muscle myosin filaments in vitro still leaves open the possibility that major structural changes in the filaments may occur in vivo upon activation. Furthermore, the morphology of the thick filaments in vertebrate smooth muscle in vivo remains unproved: some investigators favor a bipolar structure similar to that of striated muscle filaments (Ashton et al., 1975) whereas others suggest a "side-polar" (or the related "mixed-polar") structure in which crossbridge polarity does not reverse at the center of the filament, but continues along the filament length (Craig and Megerman, 1977; Hinssen et al., 1978).

Here we examine the assembly of smooth muscle myosin into a filament in vitro. Our aim is twofold: to understand how phosphorylation regulates the stability of the filament, and to determine how the structure of a smooth muscle myosin filament compares with that formed by skeletal muscle myosin. Given the overall similarity between vertebrate smooth and nonmuscle myosins (Hinssen et al., 1978), answers to these questions may well provide new insights into the assembly of myosin in a nonmuscle cell.

Structure of Minifilaments

Smooth muscle myosin isolated from turkey gizzard or calf aorta forms small, homogeneous, bipolar aggregates with low critical concentrations (<25 μg/ml) in pyrophosphate or citrate/tris buffers. By varying the citrate concentration or the pH of the pyrophosphate buffer, 15–30S minifilaments could be assembled from monomeric myosin. The size and shape of the 20–22S minifilaments (5 mM pyrophosphate, pH 7.5, or 5 mM citrate/22 mM Tris) were characterized in detail by electron microscopy and hydrodynamic techniques. This particular size filament was chosen out of the continuum, because it was possible to count the number of molecules seen in electron micrographs of metal-shadowed filaments. In larger filaments the heads were too crowded to be readily distinguished. By this approach it was estimated that the average number of molecules per 20S filament was 12–14. The number of molecules could also be estimated by combining the intrinsic sedimentation coefficient and intrinsic

viscosity in the Scheraga-Mandelkern equation (1953). By assuming a rod model (Holtzer and Lowey, 1963), a value of 9–11 molecules per filament was calculated. Given that the shape of a minifilament is not approximated particularly well by either an ellipsoid or a rod, the agreement between the hydrodynamic derived value and microscopy is better than expected. Skeletal muscle minifilaments with a comparable sedimentation coefficient were shown by a variety of biophysical methods to contain eight to nine molecules (Reisler et al., 1986*a*).

Information regarding the assembly of 20S minifilaments was obtained from inspection of the structures formed when uncross-linked minifilaments were metal-shadowed. Although it cannot be concluded that these structures are intermediates in the assembly pathway, they do highlight certain favored interactions between molecules. Antiparallel dimers that overlapped for approximately one-third the length of the myosin tail were prominent, reminiscent of a 43-nm antiparallel overlap in segments formed from smooth muscle myosin rods by precipitation with divalent cations (Kendrick-Jones et al., 1971). The importance of antiparallel interactions in the assembly of smooth muscle myosin filaments is further supported by the observation that this interaction is found in the folded 15S dimer (Trybus and Lowey, 1984). Moreover, bipolar filaments longer than 0.5 μm are generally not formed; filaments of this length or greater would have molecules that are engaged only in parallel interactions with other myosins (Craig and Megerman, 1977). Parallel dimers with a 40–50-nm axial translation were also observed, similar to those long thought to be an intermediate in the assembly of skeletal myosin filaments (Harrison et al., 1971; Davis et al., 1982).

A model for the 20–22S filament can be derived based on the observed intermolecular interactions and estimates of the number of molecules and total length of the filament. The measured bare zone length of 170–180 nm indicates nearly complete overlap of the rod in this region. The number of myosin molecules on each side of the filament can be estimated from the measured average filament length of 0.37–0.39 μm. After subtracting the contribution of the heads on both ends, the resulting filament length of 0.33–0.35 μm is consistent with three levels of crossbridges on each side staggered by 43 nm (See Fig. 6 *E* for examples of filaments with this interaction). Molecules staggered by <40 nm are certainly not excluded, but it is difficult to judge when heads are at identical levels or slightly staggered. The number of myosins at each level is also difficult to establish, but typically varies between one and three. Because the average filament has only five to seven molecules per side, it is clear that all levels cannot contain three molecules. Further growth of the filament probably increases the number of molecules at each level.

Comparison of Smooth and Skeletal Muscle Filaments

Skeletal muscle myosin minifilaments are small bipolar structures of well-defined length (~0.3 μm) and size (16–18 molecules) that sediment at 32S (Reisler et al., 1980). Smooth muscle minifilaments are similar in many respects, but form under different solvent conditions. Smooth muscle myosin polymerized over the entire pH range of 6.5–8 in 5 mM pyrophosphate, whereas chicken pectoralis myosin, like rabbit myosin (Reisler et al., 1986*b*), aggregated only in low pH pyrophosphate buffers. The difference in solubility probably reflects a different charge profile on the two types of myosins. Similarly in citrate/Tris, both smooth and skeletal myosin filaments sedimented at approximately equal rates in 2–20 mM citrate/Tris, but the shapes of the filaments, as determined by hydrodynamic and microscopic analysis, were different.

The contrast between smooth and skeletal muscle myosin minifilaments is further accentuated by the addition of salt. Oligomers of skeletal muscle myosin (tetramers and octomers) in citrate/Tris are converted to the 32S minifilament by small amounts of salt; the latter species is then relatively stable until the salt concentration exceeds ~70 mM, whereupon myosin polymerizes to form the conventional bipolar synthetic filament (Reisler et al., 1982, 1986*a*). Smooth muscle myosin does not appear to favor any particular polymeric structure, but instead forms a family of polymers whose size steadily increases as the charge is neutralized either by a drop in pH or an increase in ionic strength. This behavior is consistent with the hypothesis that electrostatic interactions are the principal determinant governing the form and length of the myosin filament (Josephs and Harrington, 1968).

In the case of skeletal muscle myosin, the 32S minifilament is considered to correspond to the more stable central region of the thick filament (Reisler et al., 1980). Titration of native filaments with salt (Trinick and Cooper, 1980; Niederman and Peters, 1982), dissociation of native filaments by water (Maw and Rowe, 1980), and kinetic experiments on assembly (Davis, 1985) all illustrate that the bare zone region is structurally more stable than the remainder of the filament. This enhanced stability has been ascribed to the antiparallel bonding present in the central region, as opposed to the parallel or polar interactions existing elsewhere in the filament. It has been proposed that strong attractive forces stabilize the antiparallel-packing, while weaker, repulsive forces limit the growth of the filament in the outer, parallel-packed regions (Davis, 1986).

The continuous distribution of smooth muscle myosin minifilaments, and the absence of synthetic filaments that can be clearly identified as bipolar, imply that antiparallel interactions are the predominant force in smooth muscle myosin filament formation. Although a specific mechanism of filament growth is not being proposed, side-polar filaments can be accounted for by assuming a stepwise addition of antiparallel dimers (possibly with a 43-nm overlap), or minifilament-like structures, which add along the direction of the filament axis. A three-dimensional filament could be generated by adding planar layers of myosin molecules perpendicular to the filament axis (Craig and Megerman, 1977).

Effect of Phosphorylation and Nucleotide on Myosin Assembly

Perhaps the most striking difference between smooth and skeletal muscle myosin minifilaments is the effect of MgATP on the assembly of the polymer. High concentrations of the ligands ATP and pyrophosphate are able to disassemble skeletal myosin minifilaments by binding 1–2 mol of ligand to low-affinity sites on the rod (Oriol-Audit et al., 1981). Smooth muscle myosin minifilaments, provided they are dephosphorylated, require stoichiometric amounts of MgATP for complete disassembly. The effect of nucleotide is mediated entirely through the head region, in that binding to the

rod would be insignificant at these low ligand concentrations. Moreover, smooth muscle myosin rod is just as insoluble as skeletal myosin rod in the presence of nucleotide.

Phosphorylation at a single serine residue on the regulatory light chain is sufficient to overcome the solubilizing action of MgATP and stabilize the filamentous form of myosin. The small size and low critical concentration of the minifilament system make it possible to show that not only does the phosphorylated minifilament remain completely intact in the presence of MgATP, but no structural rearrangements occur in the filament. This does not imply that phosphorylated myosin is entirely indifferent to MgATP, inasmuch as the sedimentation rate of the minifilaments was slowed by the presence of nucleotide, but evidence for conformational changes within the heads cannot be inferred from such data. Upon dephosphorylation of the heads, the minifilaments immediately dissociate to a mixture of folded monomers and dimers. This disassembly is typically observed, provided the ionic strength is low and nucleotide is present. It appears that both heads need to be dephosphorylated for folding to occur, since phosphorylation of one of the two heads is sufficient to stabilize myosin in the filamentous form (Trybus and Lowey, 1985).

Although the effect of MgATP is most dramatic for smooth muscle myosin filaments, a more subtle influence can be demonstrated for skeletal muscle myosin filaments. Several recent reports emphasize the effects of MgATP on the geometry of synthetic filaments in the physiological pH range. Small amounts of MgATP were shown to reduce the diameter of synthetic filaments to that of native thick filaments (Pinset-Härström, 1985). The absence of these changes in rod aggregates suggested that MgATP acts through the head region. At much higher MgATP concentrations, Chowrashi and Pepe (1986) demonstrated a sharpening of the length distribution around 1.5 μm, which presumably is mediated by interactions occurring in the rod. Thus the effect of the MgATP on filament assembly may be a more general phenomenon than previously realized.

Conclusion

The strong preference for antiparallel interactions between smooth muscle myosin molecules observed in this study supports the view that thick filaments in smooth muscles have an inherently different structure from the bipolar filaments of skeletal muscles. Confirmation of this hypothesis must await further improvements in ultrastructural fixation techniques for visualizing the native structure. A "side-polar" filament composed of labile subunits whose interactions are modulated by phosphorylation could, however, have distinct biological advantages: such a structure would be highly adaptable for directed cellular movements in nonmuscle cells, and may be required for the unique mechanical and energetic properties of smooth muscle.

This work was supported by National Institutes of Health grants R29HL38113 to Dr. Trybus and R37AR17350 to Dr. Lowey.

Received for publication 8 July 1987, and in revised form 14 September 1987.

References

Adelstein, R. S., and C. B. Klee. 1981. Purification and characterization of smooth muscle myosin light chain kinase. *J. Biol. Chem.* 256:7501-7509.

Ashton, F. T., A. V. Somlyo, and A. P. Somlyo. 1975. The contractile apparatus of vascular smooth muscle: intermediate high voltage stereo electron microscopy. *J. Mol. Biol.* 98:17-29.

Beaven, G. H., and E. R. Holiday. 1952. Ultraviolet absorption spectra of proteins and amino acids. *Adv. Protein Chem.* 7:319-386.

Chowrashi, P. K., and F. A. Pepe. 1986. The myosin filament. XII. Effect of MgATP on assembly. *J. Muscle Res. Cell Motil.* 7:413-420.

Craig, R., and J. Megerman. 1977. Assembly of smooth muscle myosin into side-polar filaments. *J. Cell Biol.* 75:990-996.

Craig, R., R. Smith, and J. Kendrick-Jones. 1983. Light-chain phosphorylation controls the conformation of vertebrate non-muscle and smooth muscle myosin molecules. *Nature (Lond.).* 302:436-439.

Davis, J. S. 1985. Kinetics and thermodynamics of the assembly of the parallel- and antiparallel-packed sections of synthetic thick filaments of skeletal myosin: a pressure-jump study. *Biochemistry.* 24:5263-5269.

Davis, J. S. 1986. A model for length-regulation in thick filaments of vertebrate skeletal myosin. *Biophys. J.* 50:417-422.

Davis, J. S., J. Buck, and E. P. Greene. 1982. The myosin dimer: an intermediate in the self-assembly of the thick filament of vertebrate skeletal muscle. *FEBS (Fed. Eur. Biochem. Soc.) Lett.* 140:293-297.

Harrington, W. F., and S. Himmelfarb. 1972. Effect of adenosine di- and triphosphates on the stability of synthetic myosin filaments. *Biochemistry.* 11:2945-2952.

Harrison, R. G., S. Lowey, and C. Cohen. 1971. Assembly of myosin. *J. Mol. Biol.* 59:531-535.

Hinssen, H., J. D'Haese, J. V. Small, and A. Sobieszek. 1978. Mode of filament assembly of myosins from muscle and non-muscle cells. *J. Ultrastruc. Res.* 64:282-302.

Holtzer, A., and S. Lowey. 1963. On the use of the Scheraga-Mandelkern equation in determining molecular weights of very asymmetric proteins. *Biopolymers.* 1:497-500.

Josephs, R., and W. F. Harrington. 1968. On the stability of myosin filaments. *Biochemistry.* 7:2834-2847.

Kendrick-Jones, J., A. G. Szent-Györgyi, and C. Cohen. 1971. Segments from vertebrate smooth muscle myosin rods. *J. Mol. Biol.* 59:527-529.

Laemmli, U. K. 1970. Cleavage of structural proteins during the assembly of the head of bacteriophage T4. *Nature (Lond.).* 227:680-685.

Margossian, S. S., and S. Lowey. 1982. Preparation of myosin and its subfragments from rabbit skeletal muscle. *Methods Enzymol.* 85:55-71.

Maw, M. C., and A. J. Rowe. 1980. Fraying of A-filaments into three subfilaments. *Nature (Lond.)* 286:412-414.

Megerman, J., and S. Lowey. 1981. Polymerization of myosin from smooth muscle of the calf aorta. *Biochemistry.* 20:2099-2110.

Neal, M. W., and J. R. Florini. 1973. A rapid method for desalting small volumes of solution. *Anal. Biochem.* 55:328-330.

Niederman, R., and L. K. Peters. 1982. Native bare zone assemblage nucleates myosin filament assembly. *J. Mol. Biol.* 161:505-517.

Onishi, H., and T. Wakabayashi. 1982. Electron microscopic studies of myosin molecules from chicken gizzard muscle. I. The formation of the intramolecular loop in the myosin tail. *J. Biochem. (Tokyo).* 92:871-879.

Oriol-Audit, C., J. A. Lake, and E. Reisler. 1981. Structural changes in synthetic myosin minifilaments and their dissociation by adenosine triphosphate and pyrophosphate. *Biochemistry.* 20:679-686.

Perrie, W. T., and S. V. Perry. 1970. An electrophoretic study of the low-molecular-weight components of myosin. *Biochem. J.* 119:31-38.

Pinset-Härström, I. 1985. MgATP specifically controls in vitro self-assembly of vertebrate skeletal myosin in the physiological myosin pH range. *J. Mol. Biol.* 182:159-172.

Reisler, E., P. Cheung, and N. Borochov. 1986*a*. Macromolecular assemblies of myosin. *Biophys. J.* 49:335-342.

Reisler, E., P. Cheung, N. Borochov, and J. A. Lake. 1986*b*. Monomers, dimers, and minifilaments of vertebrate skeletal myosin in the presence of sodium pyrophosphate. *Biochemistry.* 25:326-332.

Reisler, E., P. Cheung, C. Oriol-Audit, and J. A. Lake. 1982. Growth of synthetic myosin filaments from myosin minifilaments. *Biochemistry.* 21:701-707.

Reisler, E., C. Smith, and G. Seegan. 1980. Myosin minifilaments. *J. Mol. Biol.* 143:129-145.

Scheraga, H. A., and L. Mandelkern. 1953. Consideration of the hydrodynamic properties of proteins. *J. Am. Chem. Soc.* 75:179-184.

Sellers, J. R., M. D. Pato, and R. S. Adelstein. 1981. Reversible phosphorylation of smooth muscle myosin, heavy meromyosin, and platelet myosin. *J. Biol. Chem.* 256:13137-13142.

Shoenberg, C. F. 1969. An electron microscope study of the influence of divalent ions on myosin filament formation in chicken gizzard extracts and homogenates. *Tissue Cell.* 1:83-96.

Small, J. V., and J. M. Squire. 1972. Structural basis of contraction in vertebrate smooth muscle. *J. Mol. Biol.* 67:117-149.

Somlyo, A. V. 1980. Ultrastructure of vascular smooth muscle. *In* Handbook of Physiology. D. F. Bohr, A. P. Somlyo, and H. V. Sparks, editors. 2nd ed., Sect. 2, Vol. II. American Physiological Society, Bethesda, MD. 33-67.

Somlyo, A. V., T. M. Butler, M. Bond, and A. P. Somlyo. 1981. Myosin filaments have non-phosphorylated light chains in relaxed smooth muscle. *Nature (Lond.).* 294:567-569.

Suzuki, H., H. Onishi, K. Takahashi, and S. Watanabe. 1978. Structure and function of chicken gizzard myosin. *J. Biochem. (Tokyo).* 84:1529–1542.

Trinick, J., and J. Cooper. 1980. Sequential disassembly of vertebrate muscle thick filaments. *J. Mol. Biol.* 141:315–321.

Trybus, K. M., T. W. Huiatt, and S. Lowey. 1982. A bent monomeric conformation of myosin from smooth muscle. *Proc. Natl. Acad. Sci. USA.* 79: 6151–6155.

Trybus, K. M., and S. Lowey. 1984. Conformational states of smooth muscle myosin: effects of light chain phosphorylation and ionic strength. *J. Biol. Chem.* 259:8564–8571.

Trybus, K. M., and S. Lowey. 1985. Mechanism of smooth muscle myosin phosphorylation. *J. Biol. Chem.* 260:15988–15995.

Tyler, J. M., and D. Branton. 1980. Rotary shadowing of extended molecules dried from glycerol. *J. Ultrastruct. Res.* 71:95–102.

Vibert, P., and R. Craig. 1982. Three-dimensional reconstruction of thin filaments decorated with a Ca^{2+}-regulated myosin. *J. Mol. Biol.* 157:299–319.

Walzthöny, D., M. Bähler, H. M. Eppenberger, T. Wallimann, and A. Engel. 1984. Unshadowed myosin molecules: STEM mass-maps of myosin heads. *EMBO (Eur. Mol. Biol. Organ.) J.* 3:2621–2626.

Yumura, S., and Y. Fukui. 1985. Reversible cyclic AMP-dependent change in distribution of myosin thick filaments in *Dictyostelium. Nature (Lond.).* 314:194–196.